HYDROLOGICAL PROCESSES
Hydrol. Process. (2012)
Published online in Wiley Online Library
(wileyonlinelibrary.com) DOI: 10.1002/hyp.9628

Coupling snowpack and groundwater dynamics to interpret historical streamflow trends in the western United States

Mohammad Safeeq,[1] Gordon E. Grant,[2]* Sarah L. Lewis[1] and Christina. L. Tague[3]

[1] *College of Earth, Ocean, and Atmospheric Sciences, Oregon State University, Corvallis, OR 97331, USA*
[2] *PNW Research Station, USDA Forest Service, Corvallis, OR 97331, USA*
[3] *Bren School of Environmental Science and Management, University of California, Santa Barbara, CA 93106-5131, USA*

Abstract:

A key challenge for resource and land managers is predicting the consequences of climate warming on streamflow and water resources. During the last century in the western United States, significant reductions in snowpack and earlier snowmelt have led to an increase in the fraction of annual streamflow during winter and a decline in the summer. Previous work has identified elevation as it relates to snowpack dynamics as the primary control on streamflow sensitivity to warming. But along with changes in the timing of snowpack accumulation and melt, summer streamflows are also sensitive to intrinsic, geologically mediated differences in the efficiency of landscapes in transforming recharge (either as rain or snow) into discharge; we term this latter factor drainage efficiency. Here we explore the conjunction of drainage efficiency and snowpack dynamics in interpreting retrospective trends in summer streamflow during 1950–2010 using daily streamflow from 81 watersheds across the western United States. The recession constant (k) and fraction of precipitation falling as snow (S_f) were used as metrics of deep groundwater and overall precipitation regime (rain and/or snow), respectively. This conjunctive analysis indicates that summer streamflows in watersheds that drain slowly from deep groundwater and receive precipitation as snow are most sensitive to climate warming. During the spring, however, watersheds that drain rapidly and receive precipitation as snow are most sensitive to climate warming. Our results indicate that not all trends in western United States are associated with changes in snowpack dynamics; we observe declining streamflow in late fall and winter in rain-dominated watersheds as well. These empirical findings support both theory and hydrologic modelling and have implications for how streamflow sensitivity to warming is interpreted across broad regions. Copyright © 2012 John Wiley & Sons, Ltd.

KEY WORDS streamflow trend; hydrologic processes; groundwater processes; climate; warming

Received 30 April 2012; Accepted 12 October 2012

INTRODUCTION

Changes in streamflow timing and magnitude have been a key research area for the past few decades. Declines in streamflow magnitude (Lins and Slack, 1999; Luce and Holden, 2009), altered flood risk (Hamlet and Lettenmaier, 2007) and earlier centroid of annual streamflow (Stewart *et al*., 2005) have been reported for the western United States. Most of these changes have been attributed to significant reductions in snowpack and earlier snowmelt, which in turn have been interpreted as primarily due to anthropogenic climate warming (Hidalgo *et al*., 2009; Barnett *et al*., 2008). Continuing warming trends in midlatitude areas (Adam *et al*., 2009; IPCC, 2007) will only intensify the focus on changes in snow accumulation and melt rate as key drivers of future effects on the hydrologic cycle (Nijssen *et al*., 2001), particularly in regions with "warm" snow packs, that is, snow accumulation occurring near 0 °C, such as the US Pacific Northwest (Nolin and Daly, 2006).

Most studies of historical changes in western US streamflow have shown an overall decline in summer flow, whereas the volume of annual streamflow has not changed much during the past 50 years. Warming-induced changes in snow accumulation and melt in lower elevation watersheds are interpreted as changing the interseasonal distribution of streamflow. Stewart *et al*. (2005), for example, showed a strong link between the start of spring snowmelt and elevation. In particular, the fraction of annual streamflow during winter has increased, whereas the summer fraction has decreased (Stewart *et al*., 2005; Regonda *et al*., 2005; Aguado *et al*., 1992; Dettinger and Cayan, 1995). Using quantile regression, Luce and Holden (2009) showed asymmetric changes in the distribution of annual flow, with greatest change in the lower quantile. Regonda *et al*. (2005) showed that spring season peak flows occurred earlier in the year in lower elevation watersheds, which was reflected in higher overall winter flow and lower flows during summer.

However, changes in snow dynamics are not the only driver of changes in streamflow. There are four primary filters (both climatic and nonclimatic) that control the shape of the hydrograph and its response to change as illustrated using a conceptual annual hydrograph (Figure 1). The annual peak of the hydrograph (Figure 1A) is primarily dependent on the amount of annual precipitation (wet year versus dry year), whereas timing and type of precipitation (rain versus snow) determine the timing of flow during the year (Figure 1B). The rate of hydrograph recession, which

*Correspondence to: Gordon Grant, PNW Research Station, USDA Forest Service, Corvallis, OR 97331, USA.
E-mail: ggrant@fs.fed.us

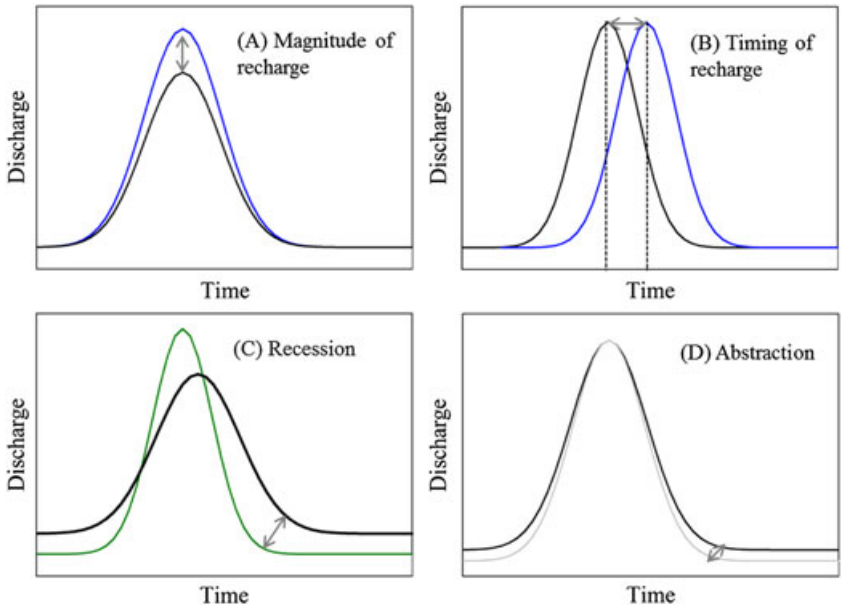

Figure 1. Conceptual annual hydrographs showing influence of individual hydrogeologic controls on the magnitude and timing of discharge. Effects of changes in climatic regime on magnitude (A) and timing (B) of recharge, (C) recession behaviour due to differences in geology between basins and (D) abstraction by vegetation. Arrows indicate the potential direction of shift in hydrograph

primarily depends on subsurface geology, controls both the portioning of subsurface water into shallow or deep pathways and affects the rate at which these compartments contribute to streamflow (Figure 1C). Factors such as aquifer permeability (as influenced by rock and rock unit porosity and fractures) and aquifer slope are the dominant means by which geology influences the recession characteristics of the hydrograph. Finally, changes in loss of water to the atmosphere in the form of evapotranspiration can also affect (increase or decrease) the hydrograph, mainly during the spring and summer growing season (Figure 1D). These four filters interact in a complex fashion to produce the hydrograph; climate affects all of these factors except the geologically mediated recession rate. The convoluted effect of these filters on hydrograph shape under different runoff regimes can be simulated using a hydrologic model (e.g. Déry *et al.*, 2009).

Recent work highlights the role of underlying geology in controlling hydrologic responses to climate change (Tague and Grant, 2009; Tague *et al.*, 2008; Arnell, 1992; Mayer and Naman, 2011; Tague and Grant, 2004). Tague and Grant (2009) propose a simple conceptual model relating sensitivity of summer streamflow to two factors: the timing of the snowmelt peak relative to late season flows and the drainage efficiency, defined as the geologically mediated rate at which recharge, either as rain or snow, is transformed into discharge. They show that, in principle, the magnitude of changes in late season streamflow will be more sensitive to later as opposed to earlier melting snowpack and more sensitive to slower as opposed to faster draining landscapes. Climate warming can potentially affect the timing of snowpack melting directly but does not alter the intrinsic drainage properties of the landscape. Interpreting sensitivity at a broad regional scale, however, requires that both factors be considered.

Building on the conceptual framework of Tague and Grant (2009), in this paper, we develop an empirical approach to examining historical trends in streamflow that incorporates both snowpack dynamics and drainage efficiency. Using long-term observed streamflow data from 81 unregulated watersheds distributed across a wide range of precipitation regimes (rain, snow and mixed) and geological settings (i.e. drainage efficiencies) in the western United States, we extract key precipitation- and streamflow-based metrics and use these to classify watersheds with respect to snowpack and drainage efficiencies. This classification then allows us to reinterpret historical trends in light of the sensitivity relationships posited by Tague and Grant (2009). The result of this analysis is a more robust means of extending forecasts of climate-driven changes in streamflow regime to watersheds without long-term observations, based on their geologies and geographic settings. Although we use streamflow records from the western United States to test these concepts, in principal this approach should work in most temperate and Mediterranean settings with strongly seasonal precipitation regimes.

GEOGRAPHY, DATA AND METHODS

Geographic area

We focused our analysis on the western United States, which is characterized by a Mediterranean climate with warm dry summers and cool wet winters, and with significant precipitation falling as snow at higher elevations. In mountainous regions, the seasonal distribution of streamflow is predominantly derived from snow, making it very sensitive to changes in temperature, as compared with elsewhere in the United States (Adam *et al.*, 2009; Nolin and Daly, 2006). Catchment characteristics such as aquifer

DOI: 10.1002/hyp

permeability and drainage efficiency differ markedly across the western United States. Streamflow recedes rapidly in watersheds with little or no spring snowmelt and limited groundwater storage (e.g. coast ranges of Washington, Oregon and northern California), resulting in high winter peaks and prolonged summer low flows. Higher elevation watersheds that receive a mix of rain and snow without much groundwater storage, such as the western Cascades of Oregon and Washington, have high winter flows, an early to midspring snowmelt peak and low summer flows. High alpine areas with little groundwater storage, such as the Sierra Nevada of California, have late spring and early summer snowmelt peaks that recede rapidly. Groundwater-dominated areas (e.g. the high Cascades of southern Washington, Oregon and northern California) are also dominated by snowmelt but show a much more uniform flow regime, with higher summer baseflows, slower recession rates and significantly lower winter peak flows.

Streamflow data

We used the high-quality daily streamflow data from 81 Model Parameter Estimation Experiment (MOPEX) gages (Schaake *et al*., 2001) located in the western United States with records extending from 1949 to 2010. MOPEX watersheds are a subset of the Hydroclimatic Data Network (HCDN) gages (Slack *et al*., 1993) and a data set compiled by Wallis *et al*. (1991). These watersheds are unregulated and span a wide variety of climate regimes (Duan *et al*., 2006). The drainage areas of watersheds examined ranged between 23 and 36599 km^2 with a median of 546 km^2 (Table A1).

WATERSHED CLASSIFICATION FRAMEWORK

On the basis of the conceptual framework posited by Tague and Grant (2009), we developed a watershed classification scheme for interpreting streamflow sensitivity to climate warming, using the precipitation regime and drainage efficiency that controls the magnitude, timing and delivery of water to stream networks. This technique required developing metrics sensitive to precipitation regime and drainage efficiency.

Metrics for precipitation regime

We used concurrent (1950–2010) 1/16 degree spatial resolution and gridded daily temperature and precipitation data for the selected study domain to characterize the precipitation regime over each watershed. The temperature and precipitation data used in this study were derived by Livneh *et al*. (2012) from the National Oceanic and Atmospheric Administration (NOAA) Cooperative Observer (Coop) stations following the gridding technique of Hamlet and Lettenmaier (2005) and are available at a 1/16 degree resolution over the CONUS domain for the period 1915–2010. Using an average temperature threshold of 0 °C, daily precipitation at each grid cell was classified as rain or snow (Jefferson, 2011). Although the temperature threshold between precipitation falling as rain versus snow varies across the study domain, 0 °C was chosen to approximate the broad regional patterns of the dominant type (rain or snow) of precipitation. For each watershed, the spatially averaged snow fraction S_f (percentage of precipitation falling as snow) was estimated using all the grid cells within the watershed boundary. On the basis of the average snow fraction for 1950–2010, watersheds were classified into three groups: (i) rain dominated ($S_f < 10\%$), (ii) mixture of rain and snow ($10\% \le S_f < 45\%$) and (iii) snow dominated ($S_f \ge 45\%$). Because our classification of watersheds based on the precipitation regime is dependent on an S_f threshold that includes the confounding effect of recent warming, we tested our classification scheme by reclassifying the watersheds based on much longer (1915–2010) temperature and precipitation data sets. If recent warming had any effect on our classification scheme, then we would expect more watersheds being classified as snow dominated compared with a mixture of rain and snow in the longer data set. The comparison showed, however, that only three watersheds changed from snow dominated to a mixture of rain and snow, and only one watershed changed from a mixture of rain and snow to snow dominated, indicating that our classification is not much affected by recent warming.

Metrics for drainage efficiency

We used the baseflow recession constant for characterizing the efficiency with which recharge becomes discharge, which is primarily a function of the watershed hydraulic conductivity and soil porosity as well as the hydraulic gradient (Sujono *et al*., 2004). After a linear reservoir model, hydrograph recession after recharge input (as snowmelt or rain) is given by

$$Q_t = Q_o e^{-kt} \quad (1)$$

where Q_t is streamflow at time t (in days), Q_o is streamflow at the beginning of the recession period, and k is a baseflow recession constant. We used k as a proxy for drainage efficiency because it reflects the rate at which water moves through the subsurface as well as the rate of recharge. There are a variety of approaches for determining k, including plotting individual recession segments on a semilogarithmic plotting graph and developing a master recession curve (Tallaksen, 1995). The recession constant k derived from individual segments varies with season and length of recession following a recharge event and may not represent the characteristic recession (Tallaksen, 1995). For this reason, we adopted the master recession curve procedure, which represents average watershed condition by combining the individual segments. It is important to recognize that k is not completely independent of recharge, particularly from snowmelt. We took steps, however, to segregate the effect of drainage efficiency versus recharge, as discussed in the following paragraph.

For the purpose of this analysis, we constructed the master recession curves for each watershed using the following approach to determine the watershed representative k:

1. We first identified all individual recession segments with length >15 days. We considered these longer recessional

DOI: 10.1002/hyp

segments to ensure the beginning of baseflow recession following recharge events.
2. The beginning of recession (inflection point) was identified following the method of Arnold *et al.* (1995) using drainage area.
3. To minimize the effect of snowmelt recharge on k, recession segments identified between the onset of the snowmelt-derived streamflow pulse and 15 August were excluded. Days of snowmelt pulse onset were determined following the method of Cayan *et al.* (2001).
4. The master recession curve was constructed using the adapted matching strip method (Posavec *et al.*, 2006), and k was determined as the slope of the linear regression between log-transformed discharge and recession length.

We discretized watersheds into two classes as follows: "low-k" watersheds with $k < 0.065$ and "high-k" watersheds with $k \geq 0.065$. We used the 0.065 threshold for k to broadly distinguish between these two major stream types. The low-k watersheds represent groundwater-dominated slow-draining systems, whereas high-k watersheds represent shallow subsurface flow-dominated fast draining systems. We acknowledge that differences in k could be caused by a variety of landscape characteristics (e.g. hydraulic gradient, relief and drainage area) other than deep versus shallow subsurface flow systems. At the scale of the western United States, however, we found no significant correlation between k and drainage area (Spearman's $r = -0.11$, $P = 0.33$) and between k and relief (Spearman's $r = -0.13$, $P = 0.26$). To further test our interpretation of k as primarily a metric of geologically mediated drainage efficiency, we correlated k with aquifer permeability for 58 (of which 13 included in this study) Oregon watersheds. The aquifer permeability data for Oregon (Wigington, *et al.*, 2012) were developed based on the correspondence between lithology (Walker *et al.*, 2003) and measured values of aquifer unit hydraulic conductivity (Gonthier, 1984; McFarland, 1983). We found a significant negative correlation between k and aquifer permeability (Spearman's $r = -0.35$, $P = 0.007$) but no correlation between k and drainage area (Spearman's $r = -0.03$, $P = 0.81$). A similar analysis from the larger population of 81 watersheds used in this study was not possible because of a lack of hydrologically relevant geologic classification for the entire western United States. Nonetheless, the k-aquifer permeability relationship in Oregon provides support for using k as a metric of geologically mediated drainage efficiency. A summary of means and corresponding standard deviations of k under different precipitation regimes (i.e. rain, mixture of rain and snow and snow) are presented in Table I.

Streamflow indices

Our evaluation of historical streamflow trends focused on variation over time of the following two indices:

1. Total streamflow (monthly, seasonal and annual): Anticipated earlier snowmelt and change in precipitation type will have a nonuniform effect on monthly and seasonal streamflow. To explore how hydrogeologic differences among the watersheds might influence changes in streamflow on varying time scales, we analyzed monthly, seasonal and annual total streamflow for trends in individual watersheds. Seasons were defined on a water year basis as fall (OND), winter (JFM), spring (AMJ) and summer (JAS).
2. Summer runoff ratio: We calculated the summer (JAS) runoff ratio for each watershed after dividing the total summer streamflow by the annual precipitation derived from PRISM data (Daly *et al.*, 2008). The average annual precipitation over a watershed was calculated from watershed averaged monthly precipitation. Trends for each watershed were calculated on the time series of the summer runoff ratio. For this index, we also calculated trends on an average time series of mean summer runoff ratio derived from n watersheds within each of the six precipitation regime and k classes.

Secular trend detection

Trends over time in the streamflow indices were estimated by the nonparametric Mann–Kendall test (Kendall, 1975; Mann, 1945) and Sen's (1968) method. The Mann–Kendall test determines whether a trend is

Table I. Characteristics of selected low-k (L) and high-k (H) watersheds, grouped by precipitation regimes as rain (R), mixture of rain and snow (M) and snow (S)

Watershed classification	No.	Hydrologic characteristic											
		Gage elevation (m)		Annual precipitation (mm)		Annual streamflow (mm)		Summer/annual streamflow (%)		Fraction of precipitation falling as snow (%)		k (day^{-1})	
		Mean	SD	Mean	SD	Mean	SD	Mean	SD	Mean	SD	Mean	SD
Low k (groundwater dominated)													
LR	5	180	190	1085	969	592	983	4	2	2.8	2.4	0.043	0.012
LM	24	394	344	1660	881	1140	879	10	5	29.3	8.2	0.041	0.019
LS	25	974	663	1398	781	930	812	20	6	59.9	10.2	0.041	0.021
High k (surface flow dominated)													
HR	9	74	62	1916	774	1366	798	3	2	3.8	2.0	0.085	0.020
HM	9	653	572	1760	814	1367	849	9	7	32.6	10.3	0.076	0.012
HS	9	950	638	1242	307	758	227	12	4	62.1	13.8	0.076	0.008

DOI: 10.1002/hyp

increasing or decreasing and estimates the significance of the trend, whereas Sen's method quantifies the magnitude of the trend. A nonparametric Kruskal–Wallis multiple comparisons test was used to test for group differences in the monthly, seasonal and water year trends by hydrogeologic regime type. A P value of 0.05 for the Kruskal–Wallis test means that the trends from at least one group of watersheds are significantly different from the trends of the other watershed types.

RESULTS

Our analysis is directed at identifying time trends in key streamflow indices in relation to underlying climatic and geologic controls. Ideally, such an analysis would clearly separate the effects of climate from geology in streamflow generation. In reality, both climate and geology are closely coupled in the streamflow signal; the hydrograph represents a complex convolution of both factors and teasing them apart is challenging. More specifically, S_f is a climate metric, reflecting the timing of precipitation input and recharge. As noted previously, k is primarily a function of watershed drainage characteristics, particularly those related to groundwater (i.e. porosity, hydraulic conductivity and hydraulic gradient) but will also be influenced to a lesser extent by the timing and magnitude of recharge (particularly snowmelt). We have attempted to minimize this effect by calculating k for periods when recharge for snowmelt and rainfall are at a minimum. Therefore, in our analysis of results, we interpret S_f as reflecting the climatic regime (and therefore sensitive to warming effects), whereas k primarily reflects the underlying geology of the watershed.

Generalized hydrographs

The interaction between climate and geology as captured by our watershed classification framework is illuminated by a comparison of average daily flows (normalized by precipitation and watershed area) across watersheds from different climatic and geologic settings (Figures 2 and 3). Low-k rain (LR)-dominated watersheds are mainly located along the southern CA coast, whereas high-k rain (HR)-dominated watersheds are located along the OR and southern WA coast. Both LR and HR watersheds show single-peaked hydrographs during the fall and winter seasons. Despite the long recession in LR and HR watersheds, streamflow during late summer is slightly higher in LR watersheds. In contrast, low-k mixture (LM) of rain and snow and high-k mixture (HM) of rain and snow watersheds are distributed throughout the study domain and show dual-peaked hydrographs. Streamflow during summer and early fall is much higher compared with LR and HR watersheds, which can be attributed to a snowmelt peak occurring later in the year. Similar to LM and HM, low-k snow (LS) and high-k snow (HS) watersheds are also spread across the study domain and show dual-peaked hydrographs. The first peak resulting from fall and winter rain is

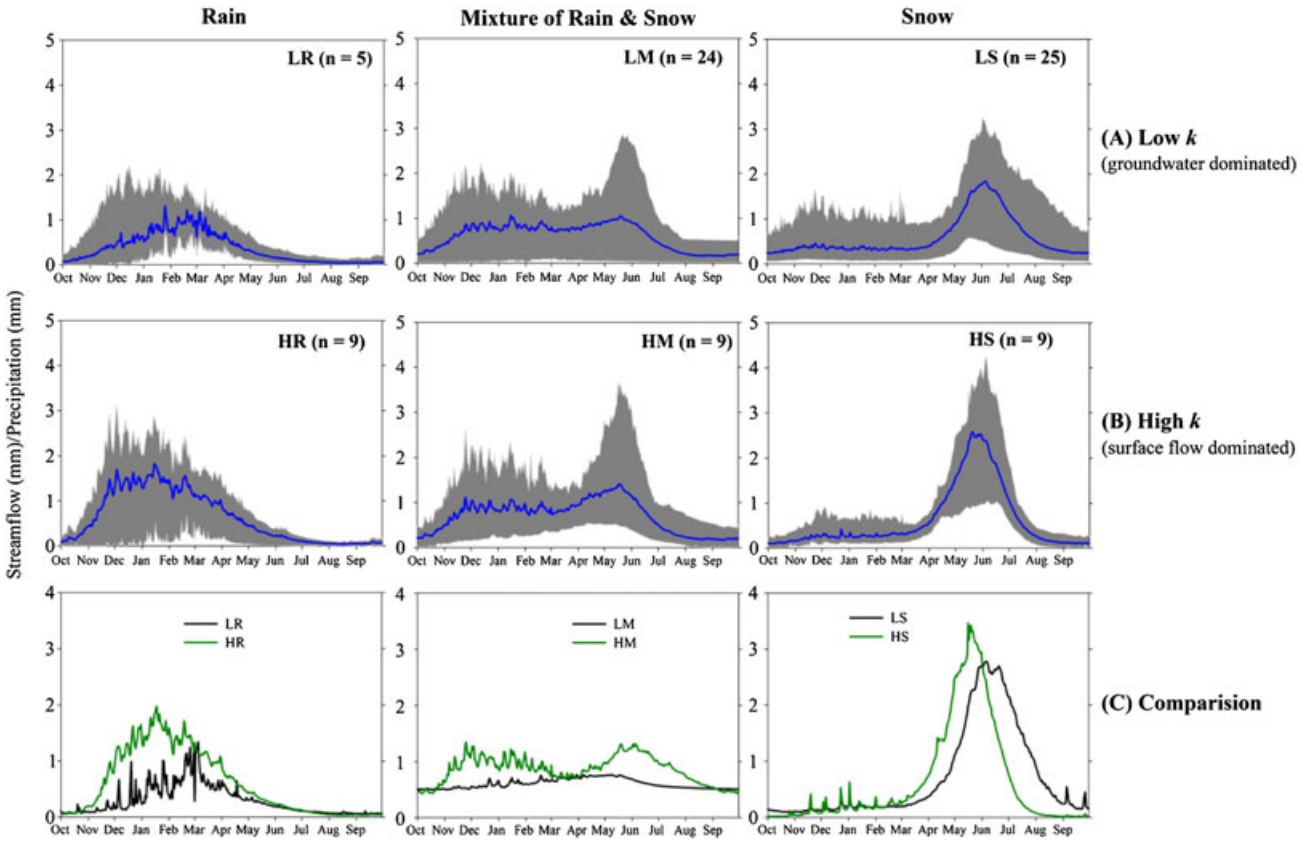

Figure 2. Ensemble average daily hydrographs for each hydrogeologic regime. Average mean daily (blue line) and range of average mean daily (gray area) streamflow for n watersheds from 1950 to 2010 shown in top (A) and middle (B) panels. The bottom panel (C) illustrates the difference in average mean daily streamflow between a low-k (black) and a high-k (green) watershed from each precipitation regime

DOI: 10.1002/hyp

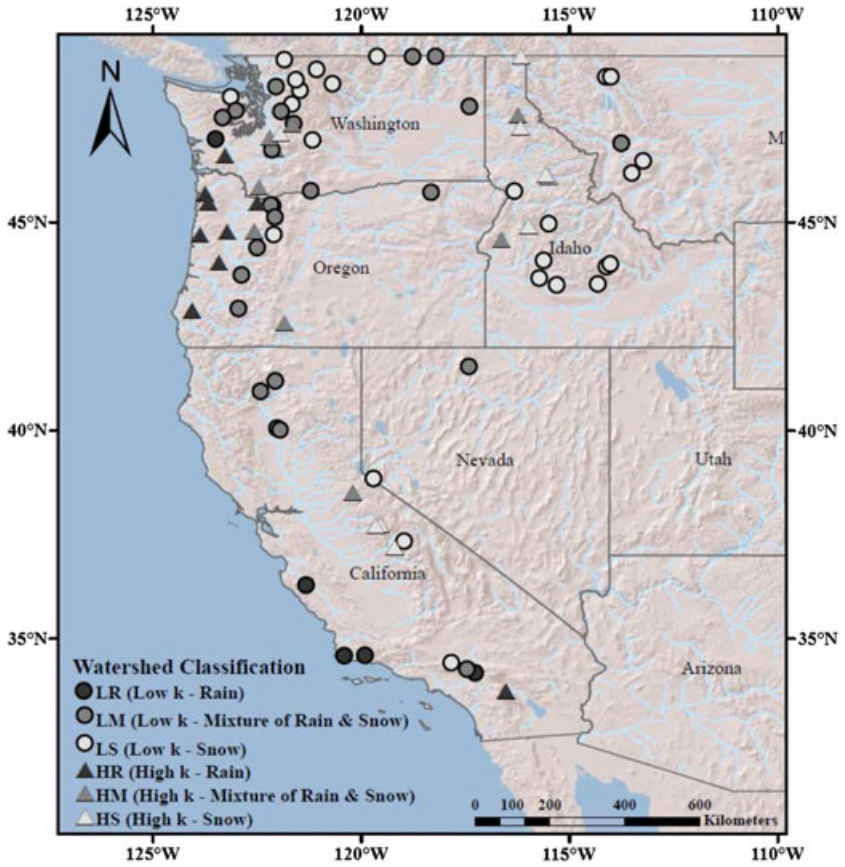

Figure 3. Study gage locations classified into hydrogeologic regime by the percentage of precipitation falling as snow (S_f) and recession constant (k)

smaller than that in LM and HM watersheds. The hydrologic characteristics of study watersheds grouped in terms of S_f and k are summarized in Table I. The mean annual streamflow is independent of hydrogeologic regime and depends primarily on annual precipitation. However, the percentage of annual streamflow occurring in summer is higher in low-k (groundwater-dominated) watersheds and increases with increasing S_f. Absolute summer flow is highest in watersheds with mixtures of rain and snow.

Predicting summer streamflow sensitivity from watershed classification

Combining our watershed classification scheme with the response surface derived from the conceptual model developed by Tague and Grant (2009) allows us to make first-order predictions of sensitivities of late summer (1 August) streamflow depending on the hydrogeologic regime of watersheds. Following Tague and Grant (2009), we defined sensitivity as the change in 1 August streamflow to a change in the timing of recharge or a unit change in the magnitude of recharge. Among the different hydrogeologic regimes, 1 August streamflow in LS and LM watersheds is most sensitive to unit changes in the magnitude and an earlier shift (2 weeks) in the timing of recharge (Figure 4). Under a similar precipitation regime (i.e. snow), watersheds show varying levels of sensitivity depending on k. The timing of snowmelt in LS watersheds are quite similar, except in Big Rock Creek, CA (USGS 10263500; Table A1), but summer streamflows show different levels of sensitivity to interannual variation in timing because of differences in k. On the other hand, LM watersheds have a similar range of k values as LS watersheds but show a wider range of sensitivities because of the varying timing of snowmelt. Although the timing of snowmelt in LS and HS watersheds is similar, higher k for HS watersheds makes them less sensitive.

Historical streamflow trends in relation to watershed classification

Monthly streamflow. Trends in monthly streamflow as a function of precipitation regime (rain, mixture of rain and snow and snow) and drainage efficiency (k) reveal the interaction between these two controlling factors (Figure 5). In the LR watersheds, median trends in monthly streamflow are mostly positive, except for a small decline during the months of December and January (Table II). Increases in August and October streamflow are statistically significant ($P < 0.10$) in 40% and 60% of the LR watersheds, respectively. The greatest absolute streamflow increases in LR watersheds are during the months of February and March. In contrast, LM watersheds show an overall negative trend in monthly streamflow, except for March during which the trend is significantly ($P < 0.10$) positive in 25% of the watersheds. Similarly, LS watersheds show an overall negative trend in monthly streamflow except March and April during which the trend is positive. Both the magnitude and the timing of greatest streamflow decline vary between these two (LM and LS) watershed types. In LM watersheds,

DOI: 10.1002/hyp

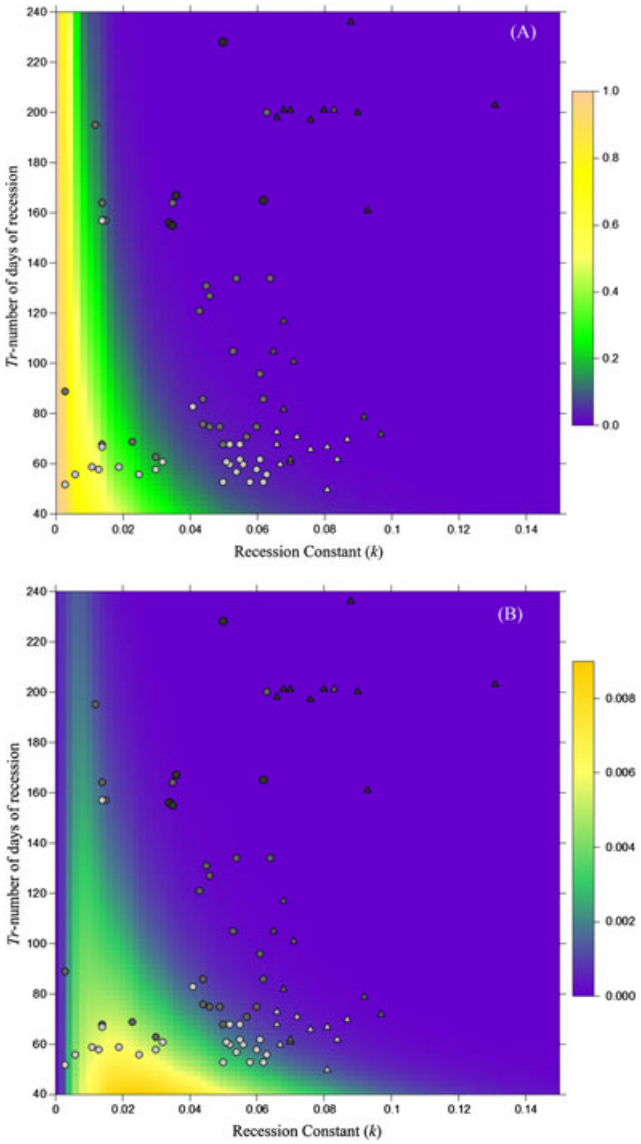

Figure 4. Response surface from conceptual model (Tague and Grant, 2009) of the sensitivity of summer streamflow to (A) a change in the magnitude of recharge and (B) an earlier shift in the timing of recharge. Assuming an initial recharge volume of 1 mm, sensitivity is represented as unit change in 1 August streamflow (mm/d), from greatest (yellow) to least (purple) sensitive. Study watersheds are represented as high-k (triangle) or low-k (circle), gray shading indicates precipitation regime from snow (light) to rain (dark)

the greatest decline is occurring during February in the winter and all months during the spring, whereas LS watersheds show the largest streamflow decline in May, June, July and August. These results indicate that both timing and magnitude of streamflow decline under a diminishing snowpack depend on the precipitation regime. Watersheds that receive precipitation mostly in the form of snow will show the greatest effect of warming during the late spring and early summer. Consistent with interpretations offered by Stewart *et al.* (2005), the increase in streamflow during March in LM watersheds and during March and April in LS watersheds can be attributed to decreasing S_f (more rain instead of snow) and earlier snowmelt.

Unlike the low-k (groundwater-dominated) watersheds, high-k watersheds (except HS watersheds) show much larger declines in monthly streamflow during fall and winter months (Table II; Figure 5). The HR watersheds show large declines between October and April with >75% watersheds showing significant ($P < 0.10$) trend in October and February. The most notable change has been in February (97 mm or 44%). These HR watersheds also show slightly larger streamflow increases between May and July compared with the corresponding LR watersheds. The mean monthly streamflow declines in HM watersheds are slightly greater compared with LM watersheds. These differences are large (nearly threefold) in October and December. In addition, HM watersheds show moderate increases in streamflow during January and much larger increases (nearly fourfold) in March. In HS watersheds, the most notable streamflow declines are in June (48 mm or 28%), which is slightly larger (in absolute terms) compared with declines in June streamflow in LS watersheds. At least 50% of the LS and HS watersheds showed a significant ($P < 0.10$) trend. Similar to HM watersheds, increases in March and April streamflow in HS watersheds are large compared with corresponding LS watersheds.

Monthly streamflow trends in rain-dominated watersheds (both LR and HR) are generally consistent with trends observed in the monthly precipitation data (Figure 6). In HR watersheds, the most notable declines in January (71 mm) and February (97 mm) streamflow are in agreement with the greatest declines in precipitation (74 mm in January and 88 mm in February). In all LR watersheds, however, the effect of significant ($P < 0.10$) increasing precipitation during February does not coincide with the month of largest streamflow increase. This can be attributed to delayed streamflow response to precipitation in groundwater-dominated (low-k) watersheds. The large increase in March streamflow in LM, HM, LS and HS watersheds does not correspond with in large decreasing trends in winter precipitation (65% of the studied watersheds showed decline in February precipitation). Hence, these trends can be attributed to changes in the type of precipitation (more rain instead of snow), consistent with a climate warming interpretation.

Historical trends as expressed as changes in the magnitude and timing of monthly streamflow are different for each of our six groups of watersheds (Figure 5). First, there is a greater change in late summer streamflow in slow-draining (low-k) LM and LS watersheds in contrast to the more rapidly draining (high-k) HM and HS watersheds. We assume that timing of recharge in HS and LS is similar; therefore, the difference in magnitude of decline is primarily due to the effect of drainage efficiency. In slow-draining (low-k) watersheds, the effect of a change in timing and magnitude of recharge gets delayed and attenuated, whereas the response to similar changes in recharge timing and magnitude in rapidly draining (high-k) watersheds will be almost immediately expressed in the hydrograph. This pattern is consistent with the results shown using the response surface from the conceptual model (Figure 4) predicting greater changes in 1 August streamflow for LS watersheds.

Monthly changes in streamflow are not limited to the summer season. The largest absolute change in historical

DOI: 10.1002/hyp

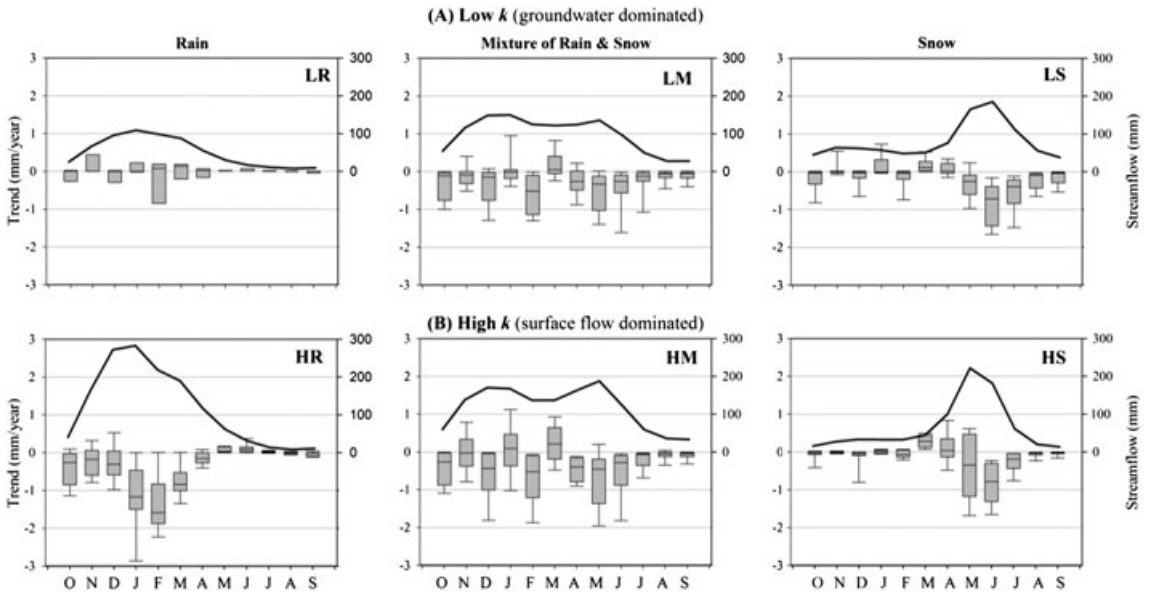

Figure 5. Average monthly streamflow (mm) and trends (mm/yr) for each hydrogeologic regime. Average monthly streamflow (solid black line) is shown on secondary *y*-axis. Trends in total monthly streamflow are shown as a box plot. The line inside the box represents the median trend between 1950 and 2010, the box itself represents the interquartile range (25th–75th percentile range) of the trends and the whiskers are the 10th and 90th percentiles of the trends. The whiskers for LR watersheds were not calculated because there are only five sites

streamflow patterns is the decline in winter streamflow in HR watersheds, a decline that is not observed in LR watersheds (Figure 5). Two factors may be responsible for these results. First, the sample size for LR watersheds is small ($n = 5$) and potentially limits interpretation. A more important factor, however, is the clear decline in precipitation in HR watersheds as compared with LR watersheds (Figure 6). This reemphasizes the point that all of the potential controls on hydrograph shape have to be taken into account in interpreting historical trends (Figure 1).

Seasonal streamflow. To accentuate seasonal patterns, we compare trends in seasonal streamflow for each group of watersheds and interpret these results in light of changing precipitation regimes among other factors (Table II). Looking at seasonal trends reveals patterns that are more easily interpreted with respect to underlying physical mechanisms than monthly totals. The LR watersheds show a trend of increasing streamflow during all seasons with the most notable change in winter (+20 mm). However, this streamflow increase is non-significant ($P > 0.10$) in all LR watersheds and only accounts for 20% of the total precipitation increase (Table III). Although spring season streamflow shows a small upward trend (+2.5 mm), spring precipitation has declined by 6 mm. In contrast, spring precipitation in LM, HR and HM watersheds has increased between 5 and 37 mm, whereas spring streamflow in these watersheds shows a negative trend (−51 to −62 mm) except HR watersheds which showed no change. These increasing trends in spring precipitation and decreasing significant ($P < 0.10$ in at least 50% of the watersheds) trends in spring streamflow in LM and HM watersheds can be attributed to reductions in snowpack for these mixed precipitation-type watersheds. For the HR watersheds, the underlying mechanisms that lead to no change in spring streamflow in response to increased precipitation are less clear. Because precipitation in HR watersheds declines by 36 mm in summer to 150 mm in winter, it may be that the effect of increased spring precipitation is negated by the water deficit caused by precipitation decline during the preceding seasons. Snow-dominated (LS and HS) watersheds show a moderate increase in winter streamflow despite the largest (90 mm in LS and 43 mm in HS) decline in winter precipitation among all seasons. Also, the decline in spring (60–106 mm) and summer (16–35 mm) season streamflow is much higher compared with the mostly nonsignificant decline in precipitation (<4 mm in spring and 8–24 mm in summer). Reduction in snowpack and earlier snowmelt under a warmer climate is responsible for nearly all the trends during the spring in snow and the mixture of rain- and snow-dominated watersheds. As a result of more winter rain instead of snow and earlier snowmelt, winter runoff ratio has increased in almost all watersheds (Figure 8), except HR, which showed decline because of large precipitation decline (Table III). LS and HS watersheds show greatest increase in winter runoff ratio as well as greatest decrease in runoff ratio during the summer.

The effect of geologic differences among watersheds is most evident in trends in summer runoff ratios (Q_{summer}/P_{annual}). All watersheds with a precipitation regime dominated by a mixture of rain and snow and only snow showed decreasing trends in summer runoff ratios, with the greater declines in slow-draining (low-*k*) watersheds (Figure 7). Declines in summer runoff ratio in snow-dominated watersheds are slightly larger than that in watersheds with precipitation regimes a mixture of rain and snow. There are no discernible trends in summer runoff ratio trends in rain-dominated watersheds. Trends in summer runoff ratio for individual watersheds are consistent with the aggregated pattern, with greatest median declines in

DOI: 10.1002/hyp

Table II. Median absolute (mm) and relative[a] (%) trends for the period 1950–2010 in total monthly, seasonal and annual streamflow for all watersheds in each hydrogeologic regime

Streamflow trend		Monthly												Seasonal				
Low k (groundwater dominated)		January	February	March	April	May	June	July	August	September	October	November	December	Fall	Winter	Spring	Summer	Annual
LR ($n=5$)	mm	−0.11	5.00	8.40	1.31	0.79	0.41	0.37	0.11†	0.00	0.27‡	0.36	−0.11	0.86	19.99	2.56	0.51	37.62
	%	−0.4	12.8	19.8	5.4	6.8	9.0	19.0	12.9	0.0	15.2	5.3	−0.7	5.3	39.9	11.0	32.1	34.5
LM ($n=24$)	mm	−1.06	−31.46‡	3.11†	−16.18†	−20.20‡	−15.90†	−7.83‡	−3.73‡	−3.4*	−6.86‡	−5.43	−8.62	−37.74†	−6.96	−51.30‡	−20.19‡	−145.40‡
	%	−0.8	−25.4	2.5	−14.3	−19.8	−22.1	−28.7	−21.4	−21.1	−26.1	−8.6	−7.4	−20.7	−1.7	−20.3	−36.2	−15.6
LS ($n=25$)	mm	−0.02	−2.37	6.62	† 0.75	−15.61	−43.46‡	−24.06‡	−5.81‡	−2.49†	−2.31†	−0.61	−1.74	−5.74	3.00	−59.54†	−34.5*	−131.54†
	%	−0.1	−13.7	27.6	1.3	−10.9	−30.2	−31.8	−18.6	−14.6	−16.4	−3.9	−9.9	−13.2	6.4	−16.7	−32.7	−22.5
High k (surface flow dominated)																		
HR ($n=9$)	mm	−71.47	−97.0*	−51.51†	−9.79	2.34	5.49†	1.38	0.11	−0.93†	−15.9*	−11.01	−19.01	−66.68	−200.70‡	0.00	0.00	−258.72†
	%	−25.3	−44.1	−27.2	−8.4	4.2	20.1	13.8	1.9	−12.3	−47.6	−6.8	−7.0	−15.0	−29.2	0.0	0.0	−18.7
HM ($n=9$)	mm	5.64	−32.02†	12.85†	−24.38†	−27.94†	−17.39†	−4.01†	−3.03†	−2.89‡	−16.34‡	−1.85	−26.58	−18.10†	3.00‡	−62.22‡	−15.13‡	−187.25†
	%	3.6	−26.3	12.3	−14.6	−16.5	−15.1	−11.9	−17.2	−11.7	−20.9	−1.3	−16.9	−5.2	0.8	−14.5	−23.9	−13.0
HS ($n=9$)	mm	0.63	−3.99	17.16‡	2.17	−20.89†	−48.10‡	−11.75	−2.40	−1.48	−2.29†	−1.09	−3.43	−8.03	9.21	*−106.10‡	−16.16‡	−159.16†
	%	3.0	−17.5	42.5	2.2	−9.7	−28.1	−20.7‡	−13.9	−12.7	−15.5	−5.4	−15.8	−17.3	12.4	−22.0	−23.6	−23.6
Kruskal–Wallis test		0.010	0.001	0.001	0.000	0.001	0.000	0.000	0.000	0.080	0.482	0.283	0.152	0.014	0.002	0.002	0.000	0.493

[a] Calculated as a percentage of median streamflow from 1950 to 2010.
*Significant trends ($P<0.1$) in at least 75% of n watersheds.
† Significant trends ($P<0.1$) in at least 25% of n watersheds.
‡ Significant trends ($P<0.1$) in at least 50% of n watersheds.

DOI: 10.1002/hyp

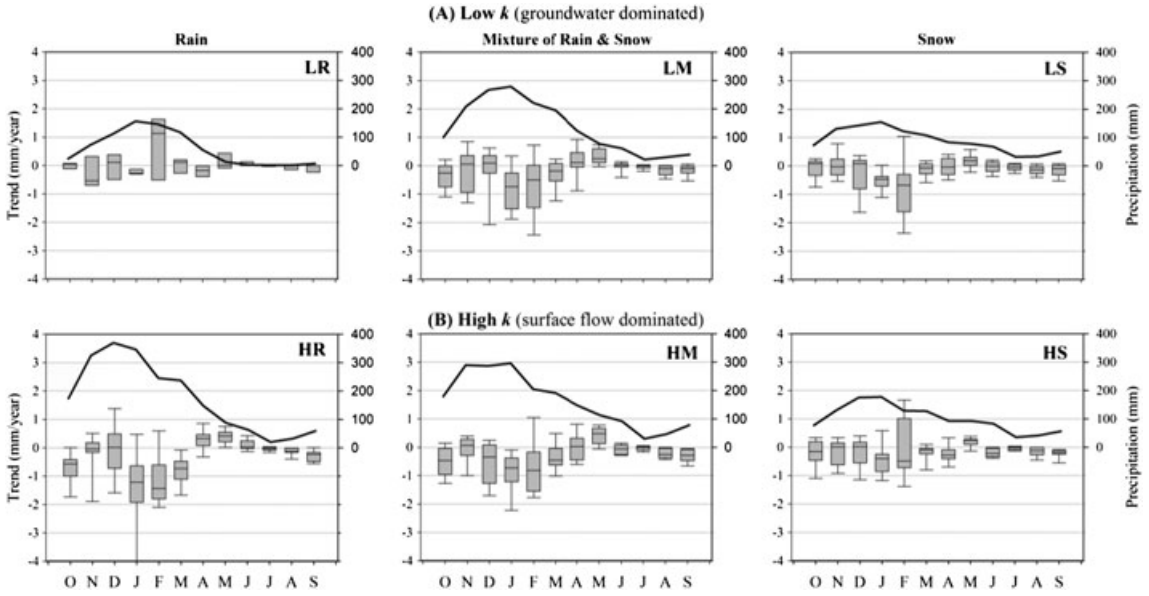

Figure 6. Average monthly precipitation (mm) and trends (mm/yr) for each hydrogeologic regime. Average monthly precipitation (solid black line) is shown on secondary *y*-axis. Trends in total monthly precipitation are shown as a box plot. The line inside the box represents the median trend between 1950 and 2010, the box itself represents the interquartile range (25th–75th percentile range) of the trends and the whiskers are the 10th and 90th percentiles of the trends. The whiskers for LR watersheds were not calculated because there are only five sites

Table III. Median absolute (mm) and relative[a] (%) trends during the period 1950–2010 in total seasonal and annual precipitation for all watersheds in each hydrogeologic regime

Precipitation trend		Seasonal				
Low *k* (groundwater dominated)		Fall	Winter	Spring	Summer	Annual
LR ($n=5$)	mm	−10.4	99.3	−5.9	0.2	54.0
	%	−4.9	23.7	−8.2	2.3	7.6
LM ($n=24$)	mm	−35.0	−65.5†	15.1	−24.1*	−102.1†
	%	−6.1	−9.3	6.8	−26.5	−6.5
LS($n=25$)	mm	−6.2	−97.0*	1.9	−23.3	−112.4†
	%	−1.9	−24.3	0.8	−20.8	−11.7
High *k* (Surface flow dominated)						
HR ($n=9$)		−18.3	−184.0*	20.1	−33.2†	−149.2
	%	−2.1	−22.6	6.8	−29.7	−6.9
HM ($n=9$)		−33.2	−68.2†	5.4	−44.1†	−108.5†
	%	−4.4	−9.9	1.5	−31.9	−5.5
HS ($n=9$)		−40.7	−43.0†	−9.1	−22.0	−95.1†
	%	−10.0	−10.0	−3.4	−16.4	−8.3

[a] Calculated as a percentage of median streamflow from 1950 to 2010.
*Significant trends ($P<0.1$) in at least 50% of *n* watersheds.
† Significant trends ($P<0.1$) in at least 25% of *n* watersheds.

LS watersheds (-3.8×10^{-3} per decade), which is nearly twofold higher than the HS watersheds ((-1.6×10^{-3} per decade). Similarly, median trends in LM watersheds (-1.8×10^{-3} per decade) were higher than those in HM watersheds (-1.2×10^{-3} per decade). Differences in trends among the six different watershed types are statistically significant ($P<0.001$).

Annual streamflow. On an annual basis, streamflow in LR watersheds increased by 38 mm in response to a 54-mm increase in annual precipitation. In the remaining watersheds, annual streamflow declined, and this decline diminishes in moving from rain- to snow-dominated watersheds. Decreasing trends were statistically significant ($P<0.10$) in 44%–50% of the watersheds. Although the decline in annual streamflow under high-*k* watersheds is higher, the Kruskal–Wallis test showed no significant difference ($P=0.49$) between the six different watershed types. Similar statistical tests on the magnitude of trends between low-*k* and high-*k* watersheds, ignoring the type of precipitation, showed no significant difference ($P=0.13$). However, in terms of runoff ratio, HS watersheds show slightly higher decline followed by LS and HR watersheds (Figure 8).

DISCUSSION AND IMPLICATIONS

Climate and climate warming directly affect the magnitude, type and timing of precipitation inputs, when water

DOI: 10.1002/hyp

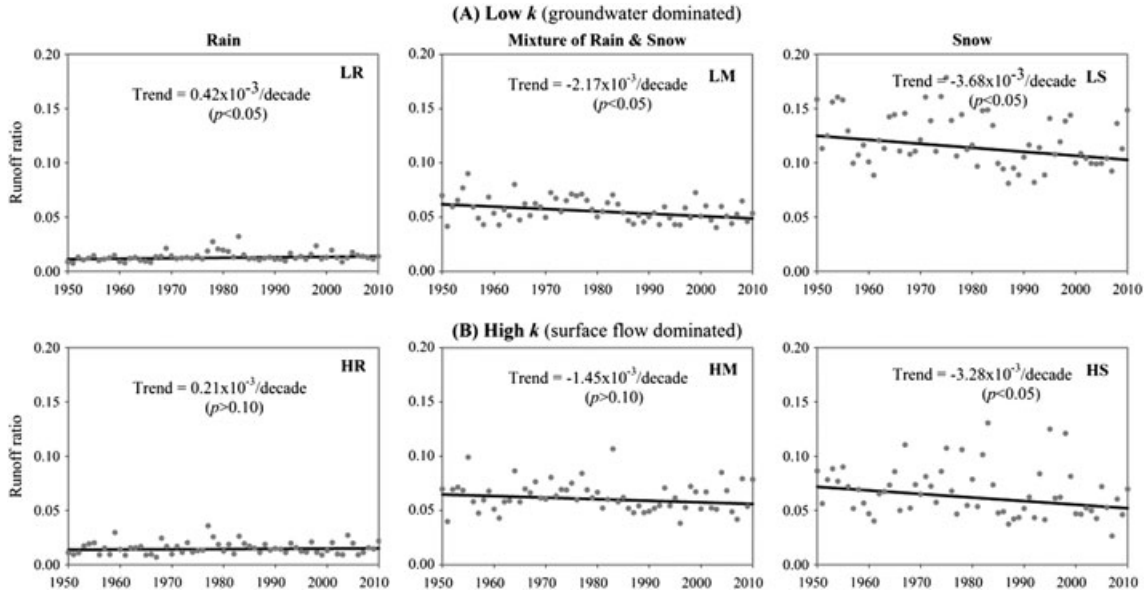

Figure 7. Temporal trends in regional average summer runoff ratios (Q_{summer}/P_{annual}) for each hydrogeologic regime

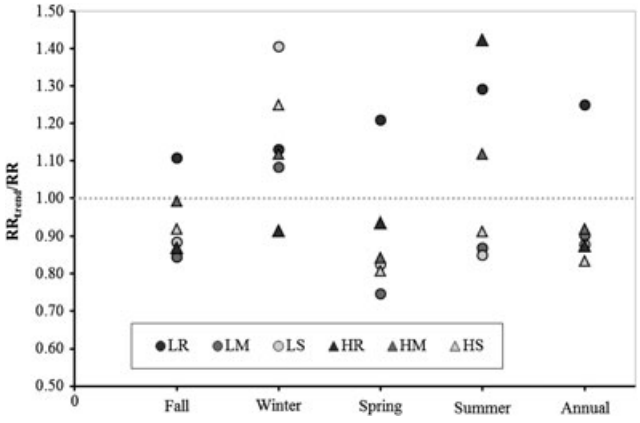

Figure 8. Long-term (1950–2010) seasonal and annual runoff ratio (RR) calculated as the ratio of median streamflow to median precipitation for each hydrogeologic regime. RR_{trend} was calculated after adding or subtracting the calculated change during the historical period (trend (mm/year) × 61 years) to the historical median streamflow and precipitation. An $RR_{trend}/RR > 1$ means increase in runoff ratio and *vice versa*

stored as snow is released as recharge, and how much water is abstracted by vegetation. The drainage efficiency of watersheds, on the other hand, is an intrinsic geological property of the landscape that is not affected by climate or warming (at least on hydrologically relevant timescales) but interacts with those factors that are influenced by climate to define the overall hydrograph and its response to climate change. All of these factors contribute to the historical trends we observe in streamflow regimes in the western United States.

Multidecade changes in streamflow regimes are not uniformly distributed across the western United States but vary systematically in both space and time with respect to process-linked controls. Changing climatic regimes are primarily expressed in terms of changes in the amount, type and timing of precipitation. The greatest decreasing trends in winter streamflow occurred in the rain-dominated watersheds (HR) and were directly associated with precipitation changes (Tables II and III). This suggests that while changes in snow dynamics can be important, trends in the magnitude and timing of precipitation as shown in earlier studies (Regonda *et al*., 2005; Mote *et al*., 2005; Pederson *et al*., 2010) and herein will be first-order controls on streamflow response. Despite the warming climate, precipitation increase (particularly in the south west) or decrease (Cascades and parts of Rockies) is the major driver of snow accumulation and melt (Mote *et al*., 2005; Pederson *et al*., 2010). The declines in fall and winter season streamflow in rain-dominated watersheds (Table II) may have contributed to the shift in flow timing toward later in the year as reported by Stewart *et al*. (2005).

Consistent with a well-founded interpretation of diminished and earlier melting snowpacks (Stewart *et al*., 2005; Mote *et al*., 2005) in snow and mixed-snow rain-dominated watersheds, the dominant hydrograph changes we report are declines in spring and summer season streamflow (Table II; Figure 5). These changes likely reflect reduced snow accumulation and earlier melt out, leading to earlier annual recessions. For areas with no net change in summer precipitation, summer streamflow in rain-dominated watersheds seems to be less sensitive than that in snowmelt-driven watersheds. These results are broadly consistent with other analyses of historical trends in streamflow from the western United States (Regonda *et al*., 2005; Stewart *et al*., 2005). However, the increase in streamflow during winter is small compared with decline in spring and summer seasons, indicating that the shift in flow timing to earlier during the water year (Stewart *et al*., 2005) is primarily driven by the decline in streamflow. In addition, monthly streamflow in the watersheds that receive precipitation in the form of a rain–snow mixture may be more sensitive than snow-dominated watersheds, particularly in late summer. This is consistent with the "snow at risk" analysis (Nolin and Daly, 2006), which identifies "warm" snow packs, that is, snow accumulation occurring near 0 °C as more sensitive to climate warming.

DOI: 10.1002/hyp

This study adds an important new dimension to the interpretation of streamflow trends, however. Our results demonstrate that broad between-watershed differences in drainage rates exert a first-order control on the magnitude of climate warming effects. In the western United States, underlying geologic controls lead to both fast shallow subsurface-dominated systems and slower deeper groundwater systems (Tague and Grant, 2009; Mayer and Naman, 2011; Tague and Grant, 2004; Jefferson *et al*., 2008). The effect of these geologically mediated spatial differences in recession characteristics on streamflow sensitivity to warming has been presented in previous theoretical and modelling studies (Tague and Grant, 2009). Here we confirm for the first time that actual streamflow trends reflect these underlying geological controls on drainage efficiency. We show that differences between "fast shallow subsurface" and "slow groundwater systems" are as important as differences between rain- and snow-dominated watersheds in evaluating streamflow response to climate change, although they are not directly affected by climate change itself. Our results show that depending on the underlying geology as reflected in k values, watersheds with similar precipitation regimes (rain and/or snow) have distinctly different hydrographs, and these differences translate into different historical trends in streamflow changes expressed over multiple decades.

Although changes in late season streamflow are particularly sensitive to geology and timing of recharge, changes in streamflow during other seasons are also important. Some of the largest changes observed, for example, were declines in fall and winter streamflow for HR watersheds, but no major changes in spring and summer streamflow (Figure 5).

Until now, hydrologic modelling has been the most common approach in understanding the hydrologic response of watersheds under climate change. However, future projections made using hydrologic models are associated with model uncertainty, which varies based on model process representation and complexity (Najafi *et al*., 2011) and spatial representation (Wenger *et al*., 2010). Our results emphasize the importance of accounting for significant differences in drainage rates that occur within the Western United States. Because drainage rates are often calibrated hydrologic parameters, this suggests that calibration strategies must explicitly account for these geologically mediated differences (Tague *et al*., 2012). Regional scale climate projections of low flows using hydrologic models that do not explicitly account for geological controls in model parameterization are likely to be erroneous. Our results may be useful in ungaged watersheds where very little or no information is available about flow regimes. By incorporating geology, which generally varies at a finer spatial scale than temperature and precipitation, areas of greater or lesser streamflow vulnerability to climate warming can be identified, at least to a first order, particularly in ungaged watersheds where models cannot be calibrated.

Climate is changing and already having demonstrable effects on the hydrology of streams across the western United States. Trends in key hydrologic variables vary across the landscape and depend not only on where "snow at risk" is located, which is widely viewed as the overarching control, but also on landscape-level variations in drainage efficiency. These differences in drainage efficiency, which are largely due to intrinsic topographic and geologic settings and factors, are not likely to change under future climates but nonetheless exert a first-order control on the magnitude and direction of climate change effects on streamflow. A more pronounced and accurate picture of where water is likely to be in the future must rely on a convolution of both extrinsic (i.e. climate) and intrinsic (i.e. drainage properties) in developing landscape-level assessments of future streamflow regimes. Similarly, management and adaptation strategies to reduce or mitigate climate effects should draw upon this broader landscape perspective.

ACKNOWLEDGEMENTS

The authors gratefully thank two anonymous manuscript reviewers for their helpful comments. They acknowledge funding support from the Oregon Watershed Enhancement Board, the Bureau of Land Management (Oregon) and the USDA Forest Service Region 6 and Pacific Northwest Research Station.

REFERENCES

Adam JC, Hamlet AF, Lettenmaier DP. 2009. Implications of global climate change for snowmelt hydrology in the twenty-first century. *Hydrological Processes* **23**(7): 962–972.

Aguado E, Cayan D, Riddle L, Roos M. 1992. Climatic fluctuations and the timing of west coast streamflow. *Journal of Climate* **5**(12): 1468–1483.

Arnell NW. 1992. Factors controlling the effects of climate change on river flow regimes in a humid temperate environment. *Journal of Hydrology* **132**(1–4): 321–342.

Arnold JG, Allen PM, Muttiah R, Bernhardt G. 1995. Automated base flow separation and recession analysis techniques. *Ground Water* **33**(6): 1010–1018.

Barnett TP, Pierce DW, Hidalgo HG, Bonfils C, Santer BD, Das T, Bala G, Wood AW, Nozawa T, Mirin AA *et al*. 2008. Human-induced changes in the hydrology of the western United States. *Science* **319** (5866): 1080–1083.

Cayan DR, Kammerdiener SA, Dettinger MD, Caprio JM, Peterson DH. 2001. Changes in the onset of spring in the western United States. *Bulletin of the American Meteorological Society* **82**(3): 399–415.

Daly C, Halbleib M, Smith JI, Gibson WP, Doggett MK, Taylor GH, Curtis J, Pasteris PA. 2008. Physiographically-sensitive mapping of temperature and precipitation across the conterminous United States. *International Journal of Climatology* **28**: 2031–2064.

Déry SJ, Stahl K, Moore R, Whitfield P, Menounos B, Burford JE. 2009. Detection of runoff timing changes in pluvial, nival, and glacial rivers of western Canada. *Water Resources Research* **45**(4): W04426.

Dettinger MD, Cayan DR. 1995. Large-scale atmospheric forcing of recent trends toward early snowmelt runoff in California. *Journal of Climate* **8**(3): 606–623.

Duan Q, Schaake J, Andréassian V, Franks S, Goteti G, Gupta HV, Gusev YM, Habets F, Hall A, Hay L *et al*. 2006. Model Parameter Estimation Experiment (MOPEX): An overview of science strategy and major results from the second and third workshops. *Journal of Hydrology* **320** (1–2): 3–17.

Gonthier JB. 1984. A description of aquifer units in eastern Oregon: U.S. Geological Survey Water-Resourcees Investigations Report 84–4095, 49.

Hamlet AF, Lettenmaier DP. 2005. Production of temporally consistent gridded precipitation and temperature fields for the continental United States. *Journal of Hydrometeorology* **6**(3): 330–336.

Hamlet AF, Lettenmaier DP. 2007. Effects of 20th century warming and climate variability on flood risk in the western U.S. *Water Resources Research* **43**(6): W06427.

Hidalgo HG, Das T, Dettinger MD, Cayan DR, Pierce DW, Barnett TP, Bala G, Mirin A, Wood AW, Bonfils C *et al*. 2009. Detection and attribution of streamflow timing changes to climate change in the western united states. *Journal of Climate* **22**(13): 3838–3855.

IPCC. 2007. *Climate change 2007*: Impacts, adaptation and vulnerability. Contribution of working group II to the fourth assessment report of the Intergovernmental Panel on Climate Change (IPCC), Parry *et al*. (eds.). Cambridge University Press. Cambridge, UK, 982.

Jefferson A, Nolin A, Lewis S, Tague C. 2008. Hydrogeologic controls on streamflow sensitivity to climate variation. *Hydrological Processes* **22** (22): 4371–4385.

Jefferson AJ. 2011. Seasonal versus transient snow and the elevation dependence of climate sensitivity in maritime mountainous regions. *Journal of Geophysical Research* **38**(16): L16402.

Kendall MG. 1975. Rank correlation methods. Griffin, London, UK.

Lins HF, Slack JR. 1999. Streamflow trends in the United States. *Journal of Geophysical Research* **26**(2): 227–230.

Livneh B, Rosenberg EA, Lin C, Mishra V, Andreadis KM, Lettenmaier DP. 2012. Extension and spatial refinement of a long-term hydrologically based dataset of land surface fluxes and states for the conterminous United States. *Journal of Climate (in review)*.

Luce CH, Holden ZA. 2009. Declining annual streamflow distributions in the Pacific northwest United States, 1948–2006. *Journal of Geophysical Research* **36**(16): L16401.

Mann HB. 1945. Nonparametric tests against trend. *Econometrica* **13**(3): 245–259.

Mayer TD, Naman SW. 2011. Streamflow response to climate as influenced by geology and elevation. *Journal of the American Water Resources Association* **47**(4): 724–738.

McFarland WD. 1983. A description of aquifer units in western Oregon, U.S. Geological Survey, Open-File Report 82-165.

Mote PW, Hamlet AF, Clark MP, Lettenmaier DP. 2005. Declining mountain snowpack in western north america. *Bulletin of the American Meteorological Society* **86**(1): 39–49.

Najafi MR, Moradkhani H, Jung IW. 2011. Assessing the uncertainties of hydrologic model selection in climate change impact studies. *Hydrological Processes* **25**(18): 2814–2826.

Nijssen B, O'Donnell G, Hamlet A, Lettenmaier D. 2001. Hydrologic sensitivity of global rivers to climate change. *Climatic Change* **50**(1): 143–175.

Nolin AW, Daly C. 2006. Mapping "at risk" snow in the Pacific northwest. *Journal of Hydrometeorology* **7**(5): 1164–1171.

Pederson GT, Gray ST, Ault T, Marsh W, Fagre DB, Bunn AG, Woodhouse CA, Graumlich LJ. 2010. Climatic controls on the snowmelt hydrology of the northern rocky mountains. *Journal of Climate* **24**(6): 1666–1687.

Posavec K, Bačani A, Nakić Z. 2006. A visual basic spreadsheet macro for recession curve analysis. *Ground Water* **44**(5): 764–767.

Ragonda SK, Rajagopalan B, Clark M, Pitlick J. 2005. Seasonal cycle shifts in hydroclimatology over the western united states. *Journal of Climate* **18**(2): 372–384.

Schaake J, Duan Q, Koren V, Hall A. 2001. Toward improved parameter estimation of land surface hydrology models through the Model Parameter Estimation Experiment (MOPEX). *IAHS Publication* **270**: 91–97.

Sen PK. 1968. Estimates of the regression coefficient based on kendall's tau. *Journal of the American Statistical Association* **63**: 1379–1389.

Slack JR, Lumb AM, Landwehr JM. 1993. Hydroclimatic data network (HCDN): A U.S. Geological Survey streamflow data set for the United States for the study of climate variation, 1874– 1988. U.S. Geological Survey Water Resources Investigation Report 93-4076.

Stewart IT, Cayan DR, Dettinger MD. 2005. Changes toward earlier streamflow timing across western north america. *Journal of Climate* **18** (8): 1136–1155.

Sujono J, Shikasho S, Hiramatsu K. 2004. A comparison of techniques for hydrograph recession analysis. *Hydrological Processes* **18**(3): 403–413.

Tague C, Grant G, Farrell M, Choate J, Jefferson A. 2008. Deep groundwater mediates streamflow response to climate warming in the oregon cascades. *Climatic Change* **86**(1): 189–210.

Tague C, Grant GE. 2004. A geological framework for interpreting the low-flow regimes of cascade streams, Willamette river basin, Oregon. *Water Resources Research* **40**(4): W04303.

Tague C, Grant GE. 2009. Groundwater dynamics mediate low-flow response to global warming in snow-dominated alpine regions. *Water Resources Research* **45**(7): W07421.

Tague CL, Choate J, Grant GE. 2012. Estimating streamflow responses to climate variability in data limited environments: The importance of hydrologic parameter uncertainty in the western Oregon cascades. *Hydrology and Earth System Sciences Discussions*. doi:10.5194/hessd-9-8665-2012.

Tallaksen LM. 1995. A review of baseflow recession analysis. *Journal of Hydrology* **165**(1–4): 349–370.

Walker GW, MacLeod NS, Miller RJ, Raines GL, Connors KA. 2003. Spatial Digital Database for the Geologic Map of Oregon, U.S. Geological Survey, Menlo Park, California.

Wallis JR, Lettenmaier DP, Wood EF. 1991. A daily hydroclimatological data set for the continental United States. *Water Resources Research* **27** (7): 1657–1663.

Wenger SJ, Luce CH, Hamlet AF, Isaak DJ, Neville HM. 2010. Macroscale hydrologic modeling of ecologically relevant flow metrics. *Water Resources Research* **46**(9): W09513.

Wigington Jr. PJ, Leibowitz SG, Comeleo RL, Ebersole JL. 2012. Oregon Hydrologic Landscapes: A Classification Framework. *Journal of the American Water Resources Association (JAWRA): 1-20*. doi: 10.1111/jawr.12009.

APPENDIX A1. LIST OF USGS GAGE STATIONS USED IN THE ANALYSIS

ID	USGS gage no.	Latitude	Longitude	Drainage area (miles^2)	Gage elevation (ft)
1	10258500	33.7450	−116.5356	93.1	700
2	10263500	34.4208	−117.8395	22.9	4050
3	10309000	38.8449	−119.7046	356.0	5000
4	10329500	41.5346	−117.4179	175.3	4700
5	11058500	34.1747	−117.2675	8.8	1590
6	11063500	34.2664	−117.4639	15.1	2605.92
7	11124500	34.5967	−119.9088	74.0	783.38
8	11132500	34.5886	−120.4085	47.1	220
9	11152000	36.2805	−121.3227	244.0	339.2
10	11230500	37.3394	−118.9735	52.5	7366.94
11	11237500	37.1986	−119.2137	22.9	7020
12	11264500	37.7316	−119.5588	181.0	4016.58
13	11266500	37.7169	−119.6663	321.0	3861.66
14	11315000	38.5191	−120.2127	21.0	5920
15	11342000	40.9396	−122.4172	425.0	1075
16	11367500	41.1882	−122.0656	358.0	2711.2
17	11381500	40.0546	−122.0242	131.0	385
18	11383500	40.0140	−121.9483	208.0	479.2
19	11501000	42.5846	−121.8497	1565.0	4202.43
20	12020000	46.6173	−123.2776	113.0	302.1
21	12035000	47.0007	−123.4949	299.0	21

(Continues)

APPENDIX A1. (Continued)

ID	USGS gage no.	Latitude	Longitude	Drainage area (miles^2)	Gage elevation (ft)
22	12048000	48.0143	−123.1327	156.0	569.3
23	12054000	47.6840	−123.0116	66.5	241.49
24	12056500	47.5143	−123.3299	57.2	762.26
25	12082500	46.7526	−122.0837	133.0	1450
26	12083000	46.7443	−122.1446	75.2	1340
27	12093500	47.0393	−122.2079	172.0	352.5
28	12098500	47.1512	−121.9498	401.0	316
29	12115000	47.3701	−121.6251	40.7	1560
30	12115500	47.3507	−121.6632	13.4	1600
31	12134500	47.8373	−121.6668	535.0	209.26
32	12149000	47.6659	−121.9254	603.0	32
33	12167000	48.2615	−122.0476	262.0	89.34
34	12175500	48.6726	−121.0729	105.0	1220
35	12186000	48.1687	−121.4707	152.0	930
36	12189500	48.4246	−121.5685	714.0	266
37	12205000	48.9060	−121.8443	105.0	1245
38	12306500	48.9992	−116.1798	570.0	2620.06
39	12330000	46.4721	−113.2340	71.3	4750
40	12332000	46.1845	−113.5025	123.0	5444.08
41	12340000	46.8997	−113.7565	2290.0	3344.76
42	12355500	48.4955	−114.1276	1548.0	3145.59
43	12358500	48.4952	−114.0101	1128.0	3128.72
44	12401500	48.9813	−118.7664	2200.0	1836.8
45	12404500	48.9843	−118.2164	3800.0	1425.5
46	12413000	47.5688	−116.2527	895.0	2100
47	12414500	47.2749	−116.1885	1030.0	2096.76
48	12431000	47.7846	−117.4044	665.0	1585.62
49	12442500	48.9846	−119.6184	3550.0	1137.7
50	12451000	48.3296	−120.6918	321.0	1098.5
51	12488500	46.9776	−121.1687	78.9	2700
52	13120000	43.9336	−114.1125	114.0	6820
53	13120500	43.9983	−114.0211	450.0	6621.95
54	13139500	43.5180	−114.3203	640.0	5295.42
55	13185000	43.6591	−115.7270	830.0	3255.7
56	13186000	43.4957	−115.3080	635.0	4218.55
57	13235000	44.0853	−115.6222	456.0	3790
58	13240000	44.9135	−115.9973	48.9	5140
59	13258500	44.5794	−116.6433	605.0	2650
60	13313000	44.9621	−115.5004	213.0	4655.75
61	13317000	45.7503	−116.3239	13550.0	1412.65
62	13336500	46.0867	−115.5139	1910.0	1540
63	13337000	46.1508	−115.5872	1180.0	1452.98
64	14020000	45.7196	−118.3233	131.0	1854.81
65	14113000	45.7565	−121.2101	1297.0	288.9
66	14137000	45.3987	−122.1284	263.0	257
67	14141500	45.4154	−122.1715	22.3	720
68	14154500	43.7360	−122.8734	211.0	856.16
69	14166500	44.0498	−123.4262	89.3	389.05
70	14178000	44.7068	−122.1012	216.0	1590.07
71	14182500	44.7915	−122.5790	112.0	655.41
72	14185000	44.3918	−122.4976	174.0	775
73	14190500	44.7832	−123.2345	240.0	171.92
74	14209500	45.1248	−122.0734	479.0	1091.69
75	14211500	45.4776	−122.5079	26.8	228.47
76	14222500	45.8368	−122.4662	125.0	356.8
77	14301000	45.7040	−123.7554	667.0	32.6
78	14301500	45.4868	−123.6876	161.0	71.89
79	14305500	44.7151	−123.8873	202.0	102.32
80	14308000	42.9304	−122.9484	449.0	991.8
81	14325000	42.8915	−124.0707	169.0	197.42

DOI: 10.1002/hyp